Phase ReLock - Localization of RFID Tags by a Moving Robot

Anastasios Tzitzis, Spyros Megalou, Stavroula Siachalou, Traianos Yioultsis, Athanasios Kehagias, Emmanouil Tsardoulias, Alexandros Filotheou, Andreas Symeonidis, Loukas Petrou, Antonis G. Dimitriou
School of Electrical and Computer Engineering, Aristotle University of Thessaloniki, Greece, e-mail: antodimi@auth.gr

***Abstract*—In this work, we propose a prototype method for the localization of RFID tags, by deploying RFID equipment on a robotic platform. The constructed robot is capable to perform Simultaneous Localization (of its own position) and Mapping of the environment and then locate the RFID tags around its path. The proposed method is based on properly treating the measured phase of the backscattered signal by each tag at the reader's antenna, located on top of the robot. More specifically, the measured phase samples are reconstructed, such that the 2π discontinuities are eliminated. This allows for the formation of an optimization problem, which can be solved rapidly by standard methods. The proposed method is experimentally compared against the most accurate reported method in prior-art and the same accuracy is preserved. However, the problem is solved more than one order of magnitude faster, allowing for the applicability of the method in real-time inventorying and localization.**

***Index Terms*—RFID, Localization, Robotics, SLAM, Optimization.**

I. Introduction

This work aims at automatic inventorying and accurate, real-time localization, by deploying a moving robot (see Fig. 1). The robot carries RFID equipment (reader, antenna) and a combination of sensors (lidar, depth cameras) to perform Simultaneous Localization (of the robot) and Mapping (of the area); also known as SLAM, [1]. Passive RFID tags are attached to each object of interest. Representative applications could include warehouse-management or large retail stores. Each tag backscatters its unique ID, which is associated with the attached object. We wish to identify and locate the position of the tag. The proposed solution exploits ***mobility*** to reduce the overall cost of an equivalent inventorying solution, consisting of readers and antennas at fixed locations.

An additional advantage of the proposed system, is its potential to reduce inaccuracies, due to multipath fading [2]. In contrast to a fixed installation of antennas and readers, a moving robot provides many measurements at successive, closely-spaced locations, thus allowing to stochastically treat fading effects due to multipath [3]. This wealth of measurements collected by a single moving antenna is often called as "virtual antenna array" in related prior art.

To the best of our knowledge, this is the first time that the actual problem is realistically treated; both the locations of the robot (i.e. the reader-antennas) and the tags are unknown and must be evaluated. Prior-art treats those problems separately; RFID-tag localization algorithms consider the location of the reader-antenna as known [4], while SLAM algorithms aim only at localizing the robot. In this work, we focus on the localization method of the RFID-tags, while the path of the robot is estimated and updated by a SLAM algorithm.

Localization techniques exploit the measured phase and back-scattered power of each tag at the reader-antenna pair located on the robot. Depending on the treatment of this information, we have direction-finding techniques, [5], [6], "fingerprinting" methods, [7], [8], "holographic" methods, [9]-[11], conditional probability based methods [12]-[16] and other techniques [17]. Some may involve custom RFID-readers, [8], [17], usually Software Defined Radio transceivers, or out-of-band emissions [17]. Among the techniques that promise best accuracy with commodity RFID hardware (off the shelf components) are those based on exploiting the phase of the backscattered electromagnetic (EM) field and mainly the holographic method, or its differential variations, [9]-[11]. The holographic method demands for an exhaustive search of all possible tag locations to identify the one that maximizes a given cost function. However, despite of its high accuracy, the estimation time is often prohibitive for installations, involving large tag populations.

In this work we propose a totally new approach on solving the localization problem, based on a set of measured phases. We change the optimization problem to an appropriate form that can be solved by standard optimization methods. To achieve that, we "correct" the measured phase-samples for each tag to take continuous values, instead of being constrained in 2π intervals. Then, a solution of the optimization problem is rapidly found, while the estimation accuracy is similar to the best state-of-the-art methods.

We have constructed a prototype robot, demonstrated in Fig. 1. It is able to navigate autonomously in unknown environments, produce a map of them and track any object of interest therein. Experimental measurements verify the performance of the proposed method against the holographic approach. For a 2D search space, experimental results presented herein demonstrate a 23-times improvement in the estimation time of the proposed method with respect to the holographic. Assuming a 3D search space, the corresponding improvement would increase dramatically, since the holographic search-space would be multiplied to the size of the 3rd dimension, whereas in the proposed method, the estimation-time would not increase proportionally.

In section II we present an overview of the holographic method and a detailed description of our proposed localization

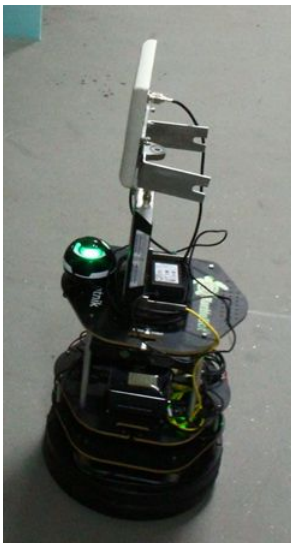

Fig. 1. The custom robot.

method. The experimental results are presented in section III and section IV concludes our findings.

II. Description of the Problem

The robot moves along a 10m-long path, e.g. inside a corridor, collecting measurements at l estimated locations with coordinates (x_i, y_i), $i = 1, \ldots, l$, as illustrated in Fig. 2. Consider that a tag t located at (x_t, y_t) is identified at $n \leq l$ antenna-locations. Let θ_{it} denote the phase measurement of the specific tag t at the i^{th} antenna pose. The measured phase at the reader is proportional to the round-trip length of the reader-to-tag-to-reader link, plus a constant phase shift, introduced by the deployed hardware, [4].

A typical curve which represents the phase measured by a moving antenna is demonstrated in Fig. 3. The x-axis of the curve represents the x-coordinate of the robot's path. The x-coordinate of the robot changes from 90cm to 435cm, since the specific tag was within reading-range of the antenna only during this part of the robot's trace. Phase ranges in $[0, 2\pi)$ intervals. Within each interval, the phase reduces as the antenna-to-tag distance reduces, and then increases as the antenna-to-tag-distance increases. When the curve changes slope, the antenna-to-tag distance is minimized; the tag should be located at a line perpendicular to the robot's trace, which crosses the (x_i, y_i) coordinates that correspond to the minimum of the phase curve.

Since the phase is measured in 2π intervals, the expected (theoretical) measurement at a reader's antenna with coordinates (x_i, y_i), for a tag placed at (x_t, y_t) shall be

$$\begin{aligned}\phi_{it}(x_t, y_t, c_t) &= \left(\frac{2\pi}{\lambda} 2d_{it} + c_t\right) \bmod 2\pi \\ &= \left(\frac{4\pi}{\lambda}\sqrt{(x_t - x_i)^2 + (y_t - y_i)^2} + c_t\right) \bmod 2\pi,\ i \in [1, n]\end{aligned} \quad (1)$$

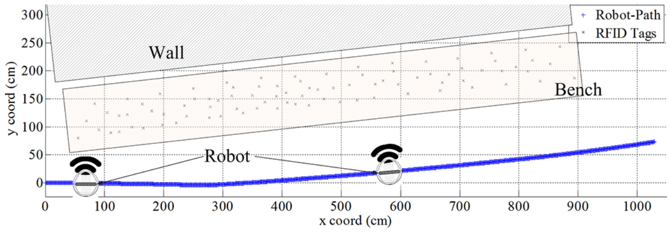

Fig. 2. Path of the robot.

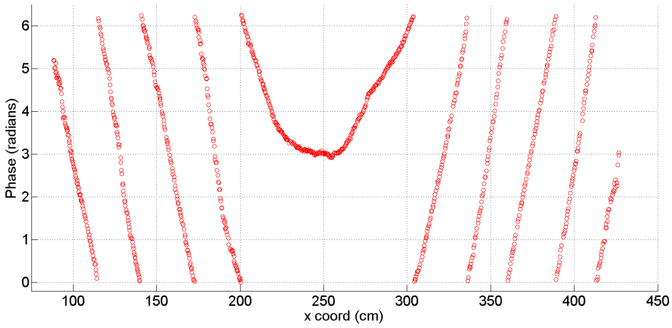

Fig. 3. Measured phase samples for a given tag.

assuming the problem is two-dimensional; i.e. the tag is at the same height as the reader's antenna. c_t represents the constant phase shift introduced by the hardware to each measured sample of the tag t. We are searching for the possible tag coordinates that fit best to the measured samples.

A. Holographic Method

The holographic method presented in [9], creates a cost function and performs an exhaustive search on all possible tag locations in the space of interest to find the one that best matches the observations/measurements. Let a grid of m possible locations of the unknown tag. For any possible location (x_k, y_k) of the grid the following cost function-term is calculated:

$$P_k = \left| \sum_{i=1}^{n} e^{j(\theta_{it} - \phi_{ik})} \right|, \quad k = 1, \ldots, m \quad (2)$$

In (2), θ_{it} corresponds to the measured phase-sample of "target" tag t from the robot's coordinates (x_i, y_i) and ϕ_{ik} is the theoretical/expected phase value that would have been measured if the tag was located at position (x_k, y_k), from the same robot's coordinates (x_i, y_i). At a location near the actual tag position, these vectors are expected to add constructively, whereas at distant locations they will add randomly resulting in a much lower sum. According to this method, the coordinates of the tag are estimated by maximizing (2).

The method is expected to ensure high accuracy, but can be time-consuming. The number of calculations involved is proportional to the size and density of the search space and for large problems and especially three-dimensional problems the estimation-time can be greatly increased.

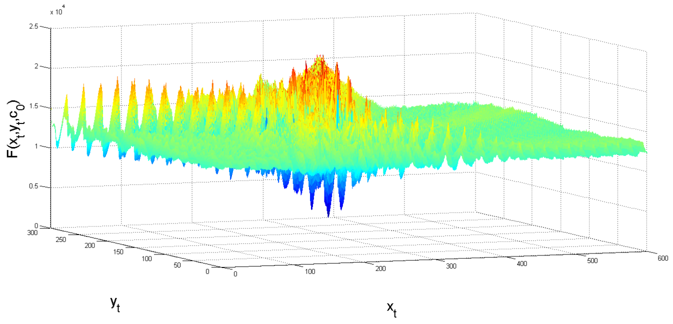

Fig. 4. Non convex objective function $F(x_t, y_t, c_{t,0})$ for a constant $c_{t,0}$.

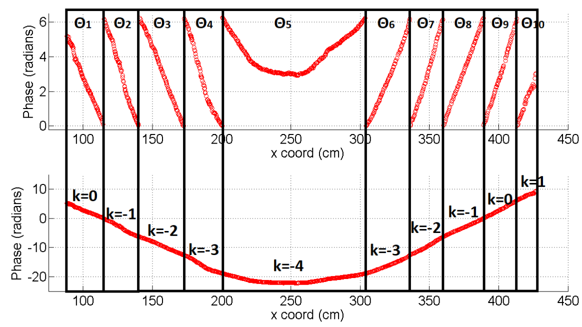

Fig. 5. Reconstruction of the measured phase samples.

B. Proposed Method

Our goal is to create an appropriate cost/objective function, which can be optimized by standard optimization algorithms that promise rapid execution. Treating the above as an optimization problem, we are searching for the best selection of parameters (x'_t, y'_t, c'_t) that minimize the following function:

$$F(x_t, y_t, c_t) = \sum_{i=1}^{n} \left[\phi_{it}(x_t, y_t, c_t) - \theta_{it}\right]^2 = \sum_{i=1}^{n}[((\tfrac{4\pi}{\lambda}\sqrt{(x_t - x_i)^2 + (y_t - y_i)^2} + c_t) \bmod 2\pi - \theta_{it}) \bmod 2\pi]^2 \tag{3}$$

The pair (x'_t, y'_t) corresponding to the global minimum of (3) is the solution of the proposed algorithm.

The objective function $F(x_t, y_t, c_t)$ is nonlinear and should be minimized by applying a nonlinear optimization/fitting method. Such methods involve mostly iterative algorithms [18]. They start from an initial selection of the parameters and adjust them by exploiting certain information; e.g. the values of first or second derivatives, so that the objective function value decreases. The procedure shall be repeated until some specified convergence criteria are met. State-of-the-art nonlinear optimization methods, presented in [18] and [19], are based on steepest descend direction, Newton's direction, Line search, Trust Region, etc. In general, iterative algorithms converge to a local minimum of the objective function. However, optimization, by its definition, means finding the best solution overall and therefore ideally, algorithms should converge to the *global minimum*. This can be assured when convex objective functions are involved [20]; i.e. functions with one and only global minimum.

In our case, due to the repetitive form of both the curve of the expected phase values and the curve of the measured phase samples, the objective function (3) tends to have a repetitive-shaped curve, too, as shown in Fig. 4. As a consequence, it is not convex and has many local minima (and maxima). Any fitting algorithm would be trapped around one of them, instead of converging to the optimum solution.

C. Phase ReLock

We propose a post-processing of the phase measured samples so that the ***global minimum*** of the new objective function can be rapidly found by common optimization techniques. The aforementioned processing refers to the reconstruction of the phase curve in order to obtain a continuous form, eliminating the discontinuities every 2π. The proposed method is called **Phase ReLock**.

Initially, we detect the discontinuities of the curve and distinguish every 2π interval in it. Let $\boldsymbol{\Theta_j}$ be the set of the phase samples corresponding to the j^{th} out of m 2π intervals. Each $\boldsymbol{\Theta_j}$ represents a specific part of the phase-curve as shown in Fig. 5 (top). Each of these parts should be shifted along the phase-axis according to:

$$\boldsymbol{\Theta'_j} = \boldsymbol{\Theta_j} + k_j \cdot 2\pi,\ \ j = 1, ..., m, \tag{4}$$

where $k_j \in Z$ and it's calculated so that a continuous curve is produced and any discontinuity between successive measurements is eliminated (see Fig. 5 - bottom).

Now the theoretical function (1) changes to:

$$\begin{aligned}\phi'_{it}(x_t, y_t, c_t) &= \left(\frac{2\pi}{\lambda}2d_{it} + c_t\right) \\ &= \left(\frac{4\pi}{\lambda}\sqrt{(x_t - x_i)^2 + (y_t - y_i)^2} + c_t\right),\ \ i = 1, .., n\end{aligned} \tag{5}$$

and the new cost function is written as:

$$\begin{aligned}F'(x_t, y_t, c_t) &= \sum_{i=1}^{n} \left[\phi'_{it}(x_t, y_t, c_t) - \theta'_{it}\right]^2 \\ &= \sum_{i=1}^{n}\left[\left(\frac{4\pi}{\lambda}\sqrt{(x_t - x_i)^2 + (y_t - y_i)^2} + c_t\right) - \theta'_{it}\right]^2\end{aligned} \tag{6}$$

where θ'_{it} is the processed measured phase sample corresponding to the "target" tag t from antenna's coordinates (x_i, y_i). One can notice that (5) and (6) are same as (1) and (3) respectively; the only difference being that the operation of modulus is now removed.

The new objective function $F'(x_t, y_t, c_t)$ no longer suffers from local minima (see Fig. 6). Therefore, an optimization algorithm (e.g. [21]) can be applied to find the optimum parameters (x'_t, y'_t, c'_t) that correspond to the global minimum of (6). In this way, the unknown location of the tag t is estimated. The resemblance between the reconstructed measured phase curve and the curve produced by (5) for the best (x'_t, y'_t, c'_t) is shown in Fig. 7.

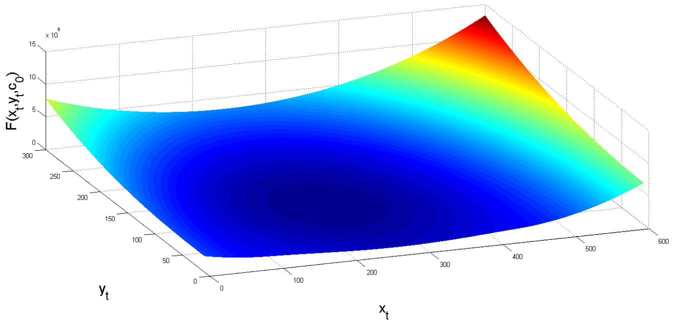

Fig. 6. Objective function $F'(x_t, y_t, c_{t,0})$ for a constant $c_{t,0}$, after the proposed reconstruction of the measured phase samples.

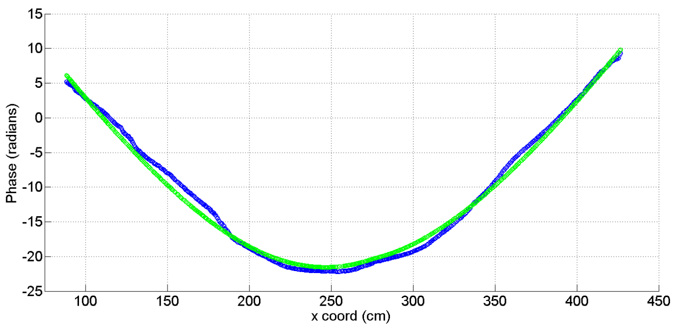

Fig. 7. Reconstructed phase-curve (blue) vs. Phase ReLock theoretical phase-curve for optimum parameters (green).

III. Experimental Results

A. Implementation

Measurements were performed, by deploying a custom robot that we constructed. We used a Turtlebot2 [22] with a Kobuki mobile base [23] for motion support, appropriately equipped to perform both RFID localization and SLAM. It carries a 7dBic "MT-242032/NRH" circularly polarized antenna from "MTI Wireless Edge" [24], connected to the Speedway Revolution R420 RFID reader [25], while the sensors responsible for the SLAM operations are an RPLidar A1 [26] and an Xtion Live Pro depth camera [27]. An Intel i7 CPU is attached to a Mini-ITX motherboard and an SSD drive for data storage.

The experiments took place in a long corridor-type laboratory room inside the Campus (see Fig. 8) and were carried out in two phases. The first phase corresponds to the operation of SLAM; the robot traverses the "a priori" unknown space and creates a map of the environment by exploiting sensor data and utilizing state-of-the-art SLAM algorithms, (e.g. [28]). In the second phase, the robot moves along a straight trajectory and it evaluates its position in the previously produced map. In the meantime, it continuously interrogates the RFID tags. The latter are placed at a millimeter-paper, forming an accurate grid on the laboratory bench (Fig. 8). The second phase was repeated 10 times for different robot's speeds and traces. As soon as the experimental implementation was finished, we compared the holographic method against the proposed "Phase ReLock".

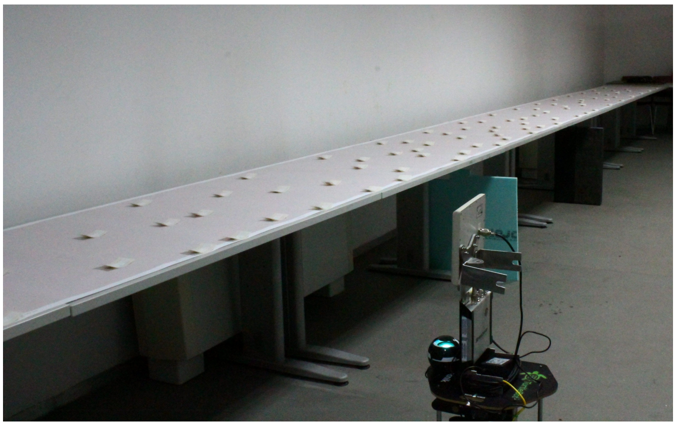

Fig. 8. Representation of the measurements's set-up.

TABLE I
EXPERIMENTAL RESULTS

Method	mean error	std	mean est-time
Phase ReLock	17.46cm	13.68cm	45.64s
Holographic	16.84cm	16.12cm	17.5min

B. Results

The holographic method was executed for a limited space around the bench; a grid of 10m length and 2m width. The locations of an average of 80 tags were estimated during each of the 10 experiments; i.e 800 estimations in total. The boxplots of the localization error for the two deployed methods are shown in Fig. 9. The mean and the standard deviation of the error and the mean estimation-time (for 80 tag evaluations) of the algorithms are given in Table I.

As far as accuracy is concerned, Phase Relock and holographic method are equivalent. They have both accomplished to locate the tags with a mean error of about $17cm$, while the standard deviation of Phase ReLock is better by $3cm$. More importantly, Phase ReLock has achieved a tremendous improvement of the algorithm speed. Localization of the tags is achieved 23 times faster than the holographic. This reduction-ratio would be further increased as the search space is increased, since the speed of the holographic depends on the size of the grid, whereas the proposed Phase ReLock doesn't. Such realistic cases demanding larger grids are three-dimensional problems.

IV. Conclusion

In this work, we have presented Phase ReLock; a prototype localization method based on the reconstruction of the phase measurements, such that standard optimization algorithms can rapidly solve the re-formed problem. Experimental results indicate comparable accuracy to the most accurate, according to prior-art, holographic method. However, we have accomplished a huge reduction of the estimation-time.

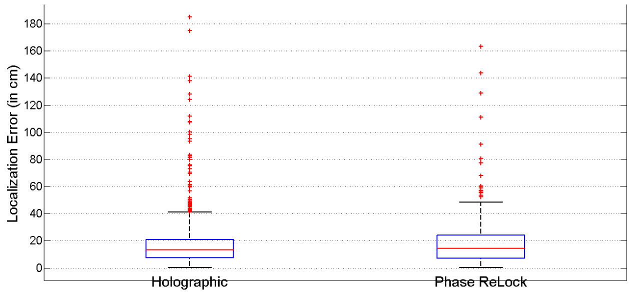

Fig. 9. Localization errors for 800 estimations.

Fig. 10. Program logo.

State-of-art localization algorithms report accuracy below 10cm, [10], but include multipath-reduction techniques involving multiple frequencies and multiple antennas, while they consider the robot-antenna positions as known. Such techniques would also improve Phase ReLock proportionally, since we achieve the same accuracy as the core localization algorithm (holographic), deployed therein [10]. In contrast to prior-art, we have considered the actual problem, where the robot must also locate itself in the map. As a result, the robot's self-localization error is "accumulated" to the localization error of the tags (since the reference positions of the reader are not exact).

Acknowledgment

This research has been co-financed by the European Union and Greek national funds through the Operational Program Competitiveness, Entrepreneurship and Innovation (Fig. 10), under the call RESEARCH – CREATE – INNOVATE (project code:T1EDK-03032).

References

[1] C. Cadena, L. Carlone, H. Carillo, Y. Latif, D. Scaramuzza, J. Neira, I. Reid, and J. J. Leonard, "Past, Present, and Future of Simultaneous Localization and Mapping: Toward the Robust-Perception Age," *IEEE Transactions on Robotics*. vol. 32, no. 6, Dec. 2016.

[2] T. Faseth, M. Winkler, H. Arthaber, and G. Magerl, "The Influence of Multipath Propagation on Phase-based Narrowband Positioning Principles in UHF RFID," *2011 IEEE-APS Topical Conference on Antennas and Propagation in Wireless Communications (APWC)*, Torino, Italy, 2011.

[3] A. G. Dimitriou, S. Siachalou, A. Bletsas, and J. N. Sahalos, "A Site-Specific Stochastic Propagation Model for Passive UHF RFID," *IEEE Antennas Wireless. Propagat. Letters*, vol. 13, pp. 623-626, Dec. 2014.

[4] P. V. Nikitin, R. Martinez, S. Ramamurthy, H. Leland, G. Spiess, and K. V. S. Rao, "Phase Based Spatial Identification of UHF RFID Tags," *2010 IEEE International Conference on RFID*, Orlando, Florida, 2010.

[5] J. Zhou, H. Zhang, and L. Mo, "Two-dimension Localization of Passive RFID Tags Using AOA Estimation," *2011 IEEE Instrumentation and Measurement Technology Conference (I2MTC)*, Binjiang, China, 2011.

[6] S. Azzouzi, M. Cremer, U. Dettmar, R. Kronberger, and T. Knie, "New Measurement Results for the Localization of UHF RFID Transponders Using an Angle of Arrival (AoA) Approach," *2011 IEEE International Conference on RFID*, Orlando (Fl), 2011.

[7] L. M. Ni, and Y. Liu, "LANDMARC: Indoor Location Sensing Using Active RFID," Wireless Networks, vol. 10, no. 6, pp. 701–710, 2004.

[8] J. Wang, and D. Katabi, "Dude, Where's my Card?: RFID Positioning that Works with Multipath and Non-line of Sight," *Proceedings of the ACM SIGCOMM 2013 conference on SIGCOMM*, pp. 51-62, Hong kong, China, 2013.

[9] R. Miesen, F. Kirsch, and M. Vossiek, "Holographic Localization of Passive UHF RFID Transponders," *2011 IEEE International Conference on RFID*, Orlando, Florida, 2011.

[10] L. Shangguan, and K. Jamieson, "The Design and Implementation of a Mobile Rfid Tag Sorting Robot," *In Proceedings of the 14th Annual International Conference on Mobile Systems, Applications, and Services*, pp. 31-42, 2016.

[11] L. Yang, Y. Chen, X.-Y. Li, C. Xiao, M. Li, and Y. Liu, "Tagoram: Real-time Tracking of Mobile Rfid Tags to High Precision Using Cots Devices," *In Proceedings of the 20th annual international conference on Mobile computing and networking*, pp. 237-248, 2014.

[12] S. Siachalou, A. Bletsas, J. N. Sahalos and A. G. Dimitriou, "RSSI-based Maximum Likelihood Localization of Passive RFID Tags Using a Mobile Cart," *IEEE Wireless Power Transfer Conference (WPTC)*, Aveiro, Portugal, 2016.

[13] S. Subedi, E. Pauls, and Y. D. Zhang, "Accurate Localization and Tracking of a Passive RFID Reader based on RSSI Measurements," *IEEE Journal of Radio Frequency Identification*, vol. 1, no. 2, pp. 144-54, 2017.

[14] J. Zhang, Y. Lyu, J. Patton, S.C. G. Periaswamy, and T. Roppel, "BFVP: A Probabilistic UHF RFID Tag Localization Algorithm Using Bayesian Filter and a Variable Power RFID Model," *IEEE Transactions on Industrial Electronics*, vol. 65, no. 10, pp. 8250-8259, 2018.

[15] F. Martinelli, "A Robot Localization System Combining RSSI and Phase Shift in UHF-RFID Signals," *IEEE Transactions on Control Systems Technology*, vol. 23, no. 5, pp. 1782-1796, 2015.

[16] P. Yang, and W. Wu, "Efficient Particle Filter Localization Algorithm in Dense Passive RFID Tag Environment," *IEEE Transactions on Industrial Electronics*, vol. 61, no. 10, pp. 5641-5651, 2014.

[17] Y. Ma, N. Selby, and F. Adib, "Minding the Billions: Ultra-Wideband Localization for Deployed RFID Tags," *MobiCom 2017, 23rd Annual Conference on Mobile Computing and Networking*, Utah, USA, 2017.

[18] V. Buljak, "Optimization Algorithms" in *Inverse Analyses with Model Reduction*, 1st Ed., 2012.

[19] K. Madsen, H. B. Nielsen, O. Tingleff, "Descent Methods" in *Methods for non-linear least square problems*, 2nd Ed., April 2004.

[20] S. Boyd, L. Vandenberghe, "Convex Optimization Problems" in *Convex Optimization*, 7th Ed. Cambridge University Press, 2009.

[21] J. J. Moré, and D. C. Sorensen, "Computing a Trust Region Step," *SIAM Journal on Scientific and Statistical Computing*, vol. 3, pp. 553–572, 1983.

[22] Turtlebot 2 Platform, Available at: http://www.turtlebot.com/turtlebot2/ (Accessed: 10 October 2018).

[23] Kobuki Mobile Base, Available at: http://kobuki.yujinrobot.com/ (Accessed: 10 October 2018).

[24] MTI Wireless Edge LTD, Available at: "http://www.mtiwe.com/ (Accessed: 10 October 2018).

[25] Impinj R420 RFID Reader, Available at: https://https://www.impinj.com/platform/connectivity/speedway-r420/ (Accessed: 10 October 2018).

[26] RPLidar sensor, Available at: https://www.slamtec.com/en/Lidar/A1 (Accessed: 10 October 2018).

[27] Xtion Live Pro Depth Camera, Available at: https://www.asus.com/gr/3DSensor/Xtion_PRO_LIVE/ (Accessed: 10 October 2018).

[28] G. Mingas, E. Tsardoulias, and L. Petrou,(2012). "An FPGA implementation of the SMG-SLAM algorithm," *Microprocessors and Microsystems*, vol. 36, no.3, pp. 190-204, May 2012